Progress In Electromagnetics Research Letters, Vol. 53, 115–119, 2015

Wideband Balun Bandpass Filter Based on Substrate Integrated Waveguide and CSRRs

Wenjie Feng*, Shunyu Yao, Jialiang Shen, and Rui Cao

Abstract—A high selectivity wideband balun bandpass filter based on substrate integrated waveguide (SIW) and complementary split rings resonators (CSRRs) is proposed. 180° reverse phase characteristic between the two output ports can be easily realized by the multi-layer SIW power divider. Eight complementary split rings resonators are used to achieve the sharp rejection upper stopband. The proposed wideband balun filter exhibits a fractional bandwidth of 37% centered at 9.45 GHz and amplitude and phase imbalance less than 0.5 dB and 1°.

1. INTRODUCTION

In recent years, the concept of substrate integrated waveguide (SIW) was proposed [1–3] to overcome the drawbacks of conventional rectangular waveguide and has drawn much attention, which takes a lot of attractive advantages such as low manufacturing cost, low profile, and easy integration process for the planar circuits. Various kinds of microwave and millimeter-wave devices based on SIW including filters, antennas, couplers, balun, and power dividers are proposed [4–7]. To further reduce the size of SIW, half-mode substrate integrated waveguide (HMSIW), folded substrate integrated waveguide (FSIW), and folded half-mode substrate integrated waveguide (FHMSIW) have also been proposed [8, 9].

As well known, balun is a three-port network and can be applied to transfer the input unbalanced signal into two output balanced signals with 180 out-of-phase difference such as in the active push-pull amplifiers, balanced mixers In the past few years, several types of baluns have emerged, e.g., Marchand balun [10, 11], power-divider balun [12], and metamaterial balun [13]. In addition, some special electromagnetic structures have been introduced to design different substrate integrated waveguide (SIW) balun and balun filter structures [14–16]. The main attentions of these structures are mainly paid to the filtering bands or the suppression of undesired spurious harmonics, and the bandwidth of the balun filter should be further extended.

In this paper, a high selectivity wideband SIW balun bandpass filter using SIW power divider [17] is proposed. Eight complementary split rings resonators (CSRRs) [18, 19] defected in the upper and bottom metal layers of the SIW power divider are used to realize the sharp rejection upper stopband with $|S_{21}|/|S_{31}|$ greater than 40 dB (12.2–13.6 GHz). A fourth-order prototype of the wideband SIW balun bandpass filter (center frequency 9.45 GHz, bandwidth 37%) can be achieved. The structure is constructed on the dielectric substrate with $\varepsilon_r = 2.65$, $h = 1.0$ mm, and $\tan\delta = 0.003$ and simulated with Ansoft HFSS v.11.

2. ANALYSIS AND DESIGN OF PROPOSED WIDEBAND SIW BALUN FILTER

As a matter of fact, SIW can be regarded as an artificial rectangular waveguide formed by two lines of periodic vias constructed into dielectric substrate, only TE_{m0} modes can be generated and propagate

Received 7 April 2015, Accepted 29 May 2015, Scheduled 2 June 2015
* Corresponding author: Wenjie Feng (fengwenjie1985@163.com).
The authors are with the Department of Communication Engineering, Nanjing University of Science & Technology, Nanjing, China.

inside, and the dominant mode is TE_{10}, the maximum value of E-field is at the vertical center plane along the propagation direction, so the center plane can be considered as an equivalent magnetic wall. An equivalent relationship between the SIW and conventional metal rectangular waveguide was derived [3] and given as below:

$$a' = \frac{2a}{\pi} \operatorname{arc\,cot}\left(\frac{\pi w}{4a} \ln \frac{w}{2d}\right) \tag{1}$$

where a' is the width of the SIW, w the distance between two adjacent cylinders, d the cylinder diameter, and a the width of the equivalent rectangular waveguide. In addition, in order to prevent the energy leakage of the SIW structure, some other conditions between d and w should be satisfied:

$$d < 0.05\lambda_g, \quad w < 2d, \quad d < 0.1a \tag{2}$$

$$\lambda_g = \lambda / \sqrt{1 - (\lambda/\lambda_c)^2} \tag{3}$$

λ_c is the cutoff wavelength of the SIW, and the cutoff frequency of the TE_{10} and TE_{20} modes in the SIW can be defined as follows [3]:

$$f_{c\mathrm{TE}_{10}} = \frac{c_0}{2\sqrt{\varepsilon_r}} \left(a' - \frac{d^2}{0.95w}\right)^{-1} \tag{4}$$

$$f_{c\mathrm{TE}_{20}} = \frac{c_0}{\sqrt{\varepsilon_r}} \left(a' - \frac{d^2}{1.1w} - \frac{d^3}{6.6w}\right)^{-1} \tag{5}$$

c_0 is the light speed in free space and ε_r the permittivity of the dielectric substrate

Figures 1(a) and (b) illustrate the 3-D view and the top view of the wideband balun bandpass filter, consisting of three layers with a metal ground located in the middle of the structure with two ports (port 2, 3) on top and bottom planes. Eight complementary split rings resonators (CSRRs) are defected in the upper and bottom layer of the SIW power divider [17]. As discussed in [17], when the signals are transmitted from port 1 to ports 2, 3, due to the 180° phase difference of the electric field at A-A' plane (as shown in Fig. 1(c)), an equal out-of-phase power division can be realized in the balanced output ports 2, 3.

The simulated results of the SIW balun without CSRRs are shown in Figs. 2(a)–(b). The power division ratio for $|S_{21}|$ and $|S_{31}|$ is less than 3.25 ± 0.2 dB with a bandwidth 62.2%, and the return loss

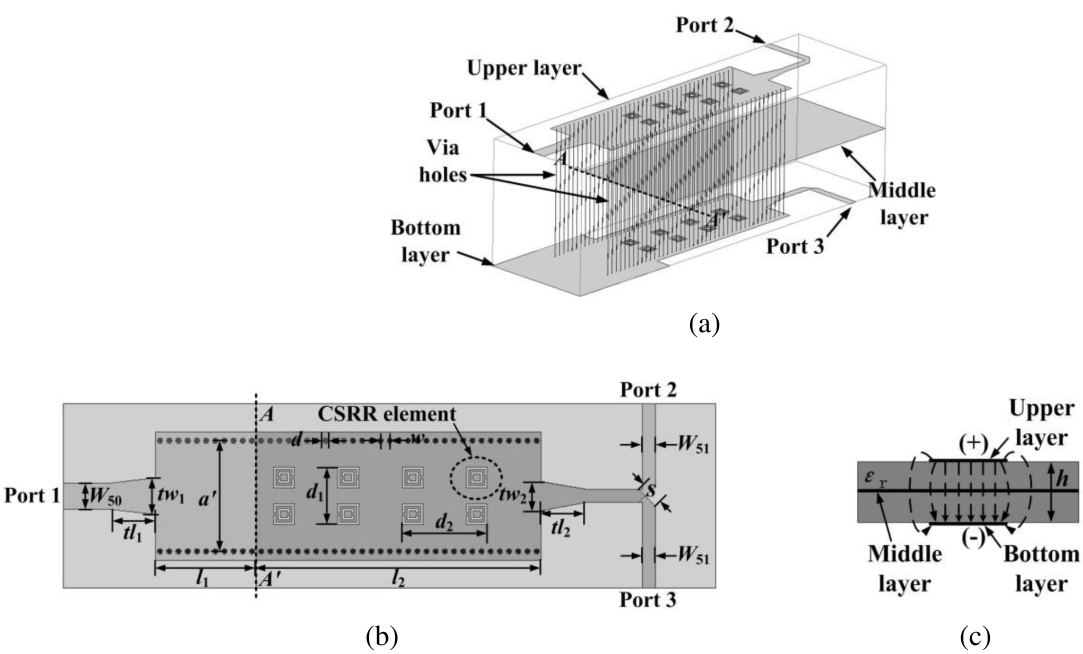

Figure 1. Structure of the wideband SIW balun filter the wideband SIW balun filter without CSRRs. (a) 3-D view of the wideband band balun filter; (b) top view of the wideband band balun filter; (c) electric field distribution at A-A' plane.

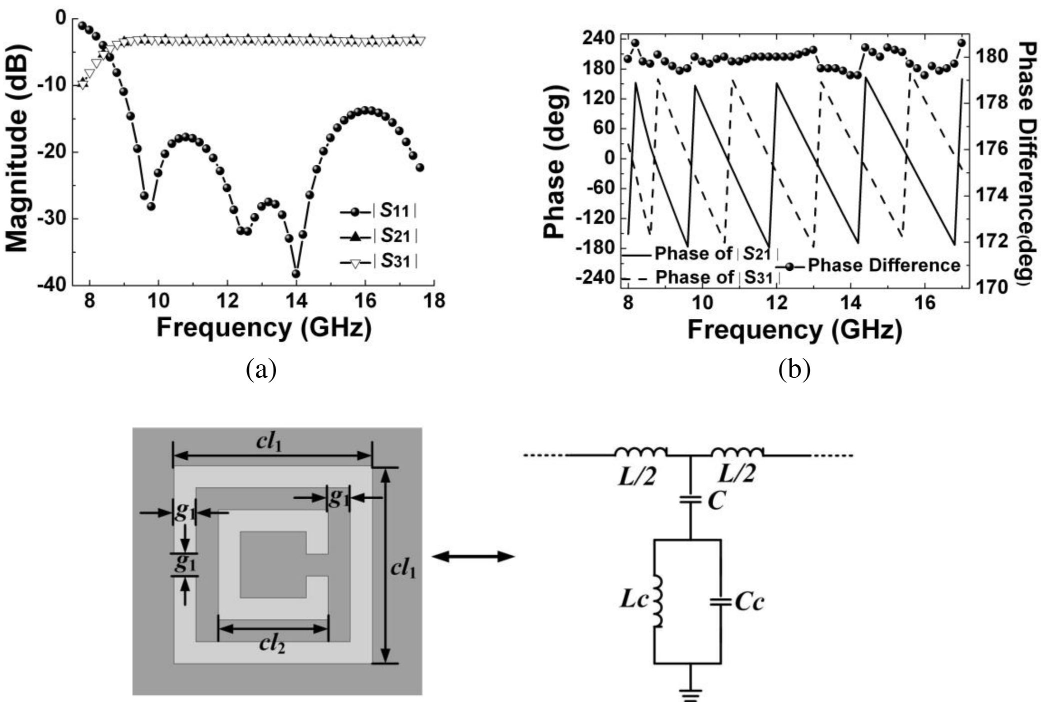

(a) (b)

(c)

Figure 2. (a) Simulated magnitudes of wideband SIW balun filter without CSRRs; (b) simulated phases of wideband SIW balun filter without CSRRs; (c) CSRR element and its equivalent circuit.

$|S_{11}|$ is greater than 15 dB (9.2–17.5 GHz). In addition, the phase difference between S_{21} and S_{31} is $180° \pm 1.5°$. In fact, the SIW power divider can be viewed as a broadband planar balun structure, and redundant via posts or longer transition are not needed in this SIW power divider. The circuit size can thus be reduced nearly 50%, and the design is much simpler than the broadband SIW planar balun (19–29 GHz, fractional bandwidth 42%) in [14].

To realize a high sharp rejection upper stopband for the SIW power divider, eight CSRRs are defected in the upper and bottom layers of the SIW power divider. The equivalent circuit of CSRR element is shown in Fig. 2(c), where the complementary split-rings resonators can be modeled by means of the resonant tank formed by the capacitance C_c and the inductance L_c. L is the inductance of the line, whereas C models the electric coupling between the line and complementary split-rings resonators. For the CSRR provides a negative effective permittivity in the vicinity of its resonant frequency, it can produce sharp rejection stop band for the SIW power divider [17]. When the slit width of the CSRR element is fixed, the resonant frequency of CSRR will increase as the inner length decreases, and when the inner length is fixed, the resonant frequency of CSRR will increase as the slit width increases [18, 19], while the CSRRs are etched in upper and bottom of the SIW power divider, and the insertion loss of the power division will become a little bigger than the original E-plane SIW power divider. The resultant dimensions of the CSRR element are given below: $cl_1 = 2.25$ mm, $cl_2 = 1.25$ mm, $g_1 = 0.25$ mm.

To clarify the proposed filter design, the design procedures of wideband balun bandpass filter are summarized as follows:

(1) Based on Equations (1)–(5), determine the width and cutoff frequency of the E-plane SIW power divider and optimize the circuit size for each metal layer.

(2) Using the formula in [18, 19], calculate the original CSRRs parameters in the upper stopband and optimize the whole SIW balun filter with three layers.

The simulated results of the wideband SIW balun bandpass filter are shown in Figs. 3(a)–(b). The cutoff frequency of dominant mode for the SIW power divider is 8.22 GHz. The simulated fractional bandwidth of the wideband balun filter is 37.1% (7.9–11.5 GHz). The minimum insertion loss is 3.7 dB for each path. A fourth-order passband with return loss greater than 13.5 dB and over 40 dB upper

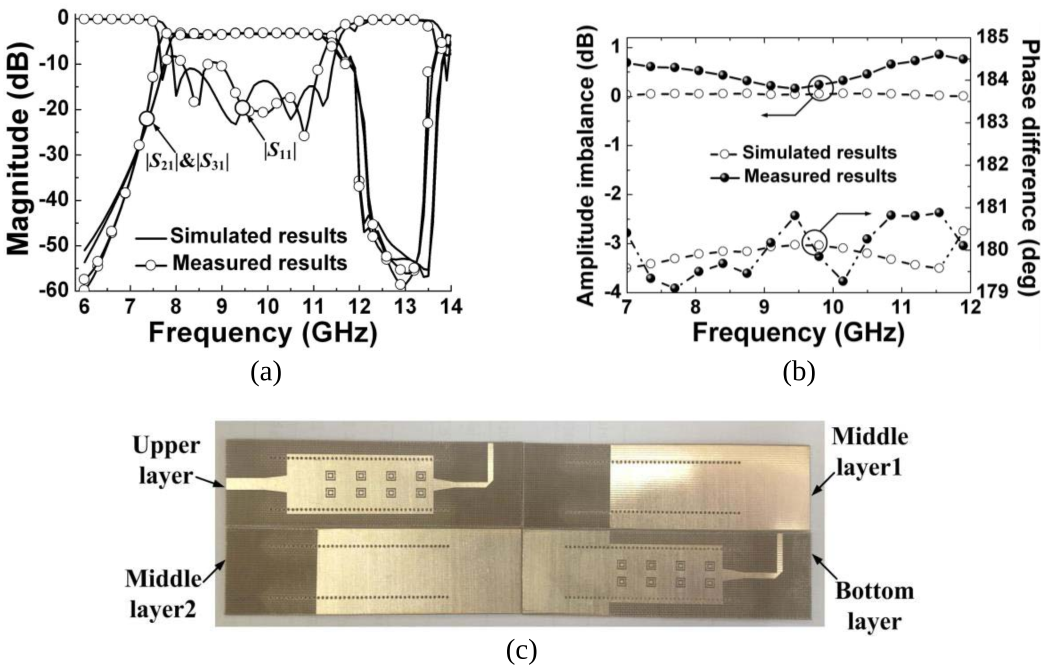

Figure 3. Measured and simulated results, photograph of the proposed SIW balun bandpass filter. (a) Measured and simulated magnitudes; (b) measured and simulated amplitude imbalance and phase difference; (c) photograph.

stopband (12.3–13.8 GHz) is thus realized. In addition, the amplitude and phase imbalances of the balun bandpass filter are less than 0.25 dB and 0.5°, respectively.

3. MEASURED RESULTS AND DISCUSSION

Figures 3(a)–(b), and (c) show the measured results and photograph of the proposed wideband SIW balun bandpass filter. The parameters of Fig. 1(a) are listed as below: $W_{50} = 2.8\,\text{mm}$, $W_{51} = 1.4\,\text{mm}$, $L_1 = 7.0\,\text{mm}$, $L_2 = 27.0\,\text{mm}$, $d_1 = 6.25\,\text{mm}$, $d_2 = 9.25\,\text{mm}$, $a = 12.0\,\text{mm}$, $d = 0.6\,\text{mm}$, $w = 1.0\,\text{mm}$, $tl_1 = 5.0\,\text{mm}$, $tw_1 = 4.0\,\text{mm}$, $tl_2 = 3.0\,\text{mm}$, $tw_2 = 5.0\,\text{mm}$, $s = 2.54\,\text{mm}$, $cl_1 = 2.25\,\text{mm}$, $cl_2 = 1.25\,\text{mm}$, $g_1 = 0.25\,\text{mm}$, $\varepsilon_r = 2.65$, $h = 1.0\,\text{mm}$, $\tan\delta = 0.003$. The measured maximum insertion loss is 4.0 dB in each path with return loss greater than 10 dB (fractional bandwidth 37%, 7.7–11.2 GHz), and over 40 dB upper stopband is obtained from 12.2 to 13.6 GHz. Moreover, the amplitude and phase imbalances in the passband of the balun bandpass filter are less than 0.5 dB and 1°. The slight frequency discrepancy for the measured results may be caused by the limited fabrication accuracy and measurement errors.

4. CONCLUSION

A compact wideband SIW balun bandpass filter with high selectivity using eight complementary split rings resonators based on a substrate integrated waveguide power divider is proposed. Equal out-of-phase power division can be easily achieved between the two balanced output ports. High selectivity, simple structure and good in-band performances can be realized for the proposed wideband SIW balun bandpass filter, indicating the validity of the design strategies.

ACKNOWLEDGMENT

This work is supported by the 2012 Distinguished Young Scientist awarded by the National Natural Science Foundation Committee of China (61225001), National Natural Science Foundation of China (6140010914), Natural Science Foundation of Jiangsu Province (BK20140791) and 2014 Zijin Intelligent Program of Nanjing University of Science and Technology.

REFERENCES

1. Hirokawa, J. and M. Ando, "Single-layer feed waveguide consisting of posts for plane TEM wave excitation in parallel plates," *IEEE Trans. Antennas Propag.*, Vol. 46, 625–630, 1998.
2. Deslandes, D. and K. Wu, "Integrated microstrip and rectangular waveguide in planar form," *IEEE Microw. Wireless Compon. Lett.*, Vol. 11, 68–70, 2001.
3. Che, W. Q., K. Deng, D. P. Wang, L. Xu, and Y. L. Chow, "Analytical equivalence between substrate-integrated waveguide (SIW) and rectangular waveguide," *IET Microw. Antennas Propag.*, Vol. 2, 35–41, 2008.
4. Cheng, Y., W. Hong, and K. Wu, "Half mode substrate integrated waveguide (HMSIW) directional filter," *IEEE Microw. Wireless Compon. Lett.*, Vol. 17, 504–506, 2007.
5. Che, W. Q., B. Fu, P. Yao, Y. L. Chow, and E. K. N. Yung, "A compact substrate integrated waveguide H-plane horn antenna with dielectric arc lens: Research articles," *Int. J. RF Microw. Comput.-Aided Eng.*, Vol. 17, 473–479, 2007.
6. Han, L., K. Wu, and S. Winkler, "Singly balanced mixer using substrate integrated waveguide magic-T structure," *Proceedings European Wireless Technology Conference*, 9–12, 2008.
7. Song, K. J., Y. Fan, and Y. Zhang, "Eight-way substrate integrated waveguide power divider with low insertion loss," *IEEE Trans. Microw. Theory Techn.*, Vol. 56, 1473–1477, 2008.
8. Hong, W., B. Liu, Y. Q. Wang, Q. H. Lai, and K. Wu, "Half mode substrate integrated waveguide: A new guided wave structure for microwave and millimeter wave application," *Proc. Joint 31st Int. Conf. Infrared Millim. Waves 14th Int. Conf. Terahertz Electron.*, 219, Shanghai, China, Sep. 18–22, 2006.
9. Che, W. Q., L. Geng, K. Deng, and Y. L. Chow, "Analysis and experiments of compact folded substrate-integrated waveguide," *IEEE Trans. Microw. Theory Techn.*, Vol. 51, 88–932, 2008.
10. Feng, W., Q. Xue, and W. Che, "Compact planar magic-T based on the double-sided parallel-strip line and the slotline coupling," *IEEE Trans. Microw. Theory Techn.*, Vol. 58, 2915–2923, 2010.
11. Feng, W. J. and W. Q. Che, "Wideband balun bandpass filter based on a differential circuit," *2012 International Microwave Symposium*, 1–3, Baltimore, Montréal, Canada, 2012.
12. Li, J. L., S. W. Qu, and Q. Xue, "Miniaturised branch-line balun with bandwidth enhancement," *IET Electron. Lett.*, Vol. 43, 931–932, 2007.
13. Xu, H. X., G. M. Wang, C. X. Zhang, and T. P. Li, "Broadband balun using fully artificial fractal-shaped composite right/left handed transmission line," *IEEE Microw. Wireless Compon. Lett.*, Vol. 22, 16–18, 2012.
14. Zhang, Z. Y. and K. Wu, "A broadband substrate integrated waveguide (SIW) planar balun," *IEEE Microw. Wireless Compon. Lett.*, Vol. 17, 843–845, 2007.
15. Wu, L. S., Y. X. Guo, J. F. Mao, and W. Y. Yin, "Design of a substrate integrated waveguide balun filter based on three-port coupled-resonator circuit model," *IEEE Microw. Wireless Compon. Lett.*, Vol. 21, 252–254, 2011.
16. Hui, J. N., W. J. Feng, and W. Q. Che, "Balun bandpass filter based on multilayer substrate integrated waveguide power divider," *IET Electron. Lett.*, Vol. 48, 571–572, 2012.
17. Feng, W. J., W. Q. Che, and K. Deng, "Compact planar magic-T using E-plane substrate integrated waveguide (SIW) power divider," *IEEE Microw. Wireless Compon. Lett.*, Vol. 20, 331–333, 2010.
18. Falcone, F., T. Lopetegi, J. D. Baena, et al., "Effective negative-stop-band microstrip lines based on complementary split ring resonators," *IEEE Microw. Wireless Compon. Lett.*, Vol. 14, 280–282, 2004.
19. Gil, I., J. Bonache, M. Gil, J. García-García, F. Martín, and R. Marqués, "Accurate circuit analysis of resonant type left handed transmission lines with inter-resonator's coupling," *J. Appl. Phys.*, Vol. 100, 1–10, 2006.